High resolution position measurement from dispersed reference interferometry using template matching

James Williamson, Haydn Martin,* and Xiangqian Jiang

University of Huddersfield, Huddersfield, UK
*h.p.martin@hud.ac.uk

Abstract: This paper describes a method to extract high resolution position data from a dispersed reference interferometry (DRI) by applying a template matching technique to the acquired spectral interferograms. Calculation of the correlation coefficient between windowed spectral interferograms acquired from the DRI apparatus and a set of numerically calculated template interferograms allows the absolute determination of position with nanometer resolution. Both the operating principle of the DRI apparatus and implementation of the template matching method is presented. Experimental validation of the method is provided through the demonstration of position tracking and an assessment of linearity, repeatability and noise performance.

OCIS codes: (120.0120) Instrumentation, measurement, and metrology; (120.3180) Interferometry; (120.6650) Surface measurements, figure; (120.5050) Phase measurement.

References and links

1. P. Hlubina, "Dispersive white-light spectral interferometry to measure distances and displacements," Opt. Commun. **212**(1-3), 65–70 (2002).
2. P. Pavlíček and G. Häusler, "White-light interferometer with dispersion: an accurate fiber-optic sensor for the measurement of distance," Appl. Opt. **44**(15), 2978–2983 (2005).
3. M. A. Galle, E. Y. Zhu, S. S. Saini, W. S. Mohammed, and L. Qian, "Characterizing short dispersion-length fiber via dispersive virtual reference interferometry," Opt. Express **22**(12), 14275–14284 (2014).
4. M. A. Galle, S. S. Saini, W. S. Mohammed, and L. Qian, "Virtual reference interferometry: theory and experiment," J. Opt. Soc. Am. B **29**(11), 3201–3210 (2012).
5. M. A. Galle and L. Qian, "Low-coherence virtual reference interferometry for dispersion analysis," IEEE Photonics Technol. Lett. **26**(20), 2020–2022 (2014).
6. P. Hlubina and I. Gurov, "Spectral interferograms including the equalization wavelengths processed by autoconvolution method," Proc. SPIE **5064**, 198–205 (2003).
7. U. Schnell, R. Dändliker, and S. Gray, "Dispersive white-light interferometry for absolute distance measurement with dielectric multilayer systems on the target," Opt. Lett. **21**(7), 528–530 (1996).
8. Y. Deng, W. Yang, C. Zhou, X. Wang, J. Tao, W. Kong, and Z. Zhang, "Wavelet-transform analysis for group delay extraction of white light spectral interferograms," Opt. Express **17**(8), 6038–6043 (2009).
9. D. Reolon, M. Jacquot, I. Verrier, G. Brun, and C. Veillas, "High resolution group refractive index measurement by broadband supercontinuum interferometry and wavelet-transform analysis," Opt. Express **14**(26), 12744–12750 (2006).
10. H. Martin and X. Jiang, "Dispersed reference interferometry," CIRP Ann. **62**(1), 551–554 (2013).
11. J. P. Lewis, "Fast template matching," Proc. Canad Imag. Proc. (Academic, 1995).
12. R. Brunelli, *Template Matching Techniques in Computer Vision: Theory and Practice* (Wiley, 2009).

1. Introduction

Over the last decade there has been an ongoing trend in the exploration of spectral interferometry (SI) for displacement and surface topography measurement, primarily because it dispenses with the need for mechanical scanning in conventional optical apparatus; a key advantage in measurement applications were measurement speed and robustness is a priority.

#258880 Received 24 Feb 2016; revised 6 Apr 2016; accepted 10 Apr 2016; published 29 Apr 2016

While there are several measurement techniques that fall into the category of SI, this paper considers advancements in what we term dispersed reference interferometry (DRI) which relies on the application of chromatic dispersion to the reference field in order to effect a wavelength dependent optical path. In DRI wide spectral interferograms are generated that feature a stationary phase point which occurs at an equalization wavelength, at which the interferometer optical path difference (OPD) is zero.

Analysis of the spectral interferograms generated allows determination of the optical path difference in absolute terms, with previously reported works across a variety of implementations demonstrating sub-micron resolutions [1, 2]. In addition to the measurement of displacement, DRI has been applied to the characterization of dispersion in fiber [3–5], transparent sample thickness measurement [6], thin film thickness measurement [7], chirped mirror characterization [8], and dispersion measurement of transparent samples [9]. This paper reports on the application of new signal processing, in the form of template matching, to increase the axial (height) measurement resolution of a previously reported DRI apparatus for measuring displacements and surface topography [10].

The authors note that DRI is referred to variously as dispersive white-light interferometry, white-light interferometry with dispersion and dispersive reference interferometry across the cited works, while spectral interferometry is used elsewhere in the literature to describe spectral analysis of interferograms more widely. As such we suggest the term dispersed reference interferometry (DRI) to refer only to those techniques that apply chromatic dispersion to the reference field [1, 2, 6, 10].

The DRI apparatus reported in this paper is based around a bulk optic Michelson interferometer sourced by a super-luminescent diode (SLD) which has a large amount of dispersion applied in the reference arm. This construction avoids limitations in an all-fiber device reported by Pavlícek and Häusler which has two independent arms, one which is formed from high dispersion fiber [2]. Modulation of the optical path length in the fiber arms through the action of temperature change and vibration means that in practical use such a device would be restricted to low precision measurement applications in the micron scale. The authors have previously demonstrated a DRI apparatus capable of an axial measurement resolution of 250 nm over a range of 200 μm with an inherently stable bulk optic setup [10]. While providing unambiguous (absolute) axial position (height) the resolution is too low for applications requiring high precision measurement. This paper reports on the extraction of high resolution phase information from the spectral interferograms acquired with the apparatus, using template matching, which enables a considerable improvement in the axial measurement resolution of DRI.

2. Principle of operation

Figure 1 shows a schematic representation of the DRI apparatus which comprises a Michelson interferometer with a chromatically dispersed reference arm. The apparatus is illuminated by a SLD source (S) having a linewidth of ~25 nm centered at 820 nm via a fibre collimator (FC) which generates an 8 mm beam diameter. The two arms of the interferometer are formed by a beamsplitter (BS). The measurement arm comprises an objective lens (L1) which focuses the light onto the measurand, which for the purposes of evaluating performance is a mirror (M1) mounted on a high-precision piezoelectric translation stage which enables movement in the axial direction. L1 has a 15 mm focal length yielding in an effective NA of ~0.26. The reference arm comprises a pair of matched transmission gratings (G1, G2), which act to introduce chromatic dispersion to the reference light after the round-trip propagation of the beam.

#258880 Received 24 Feb 2016; revised 6 Apr 2016; accepted 10 Apr 2016; published 29 Apr 2016

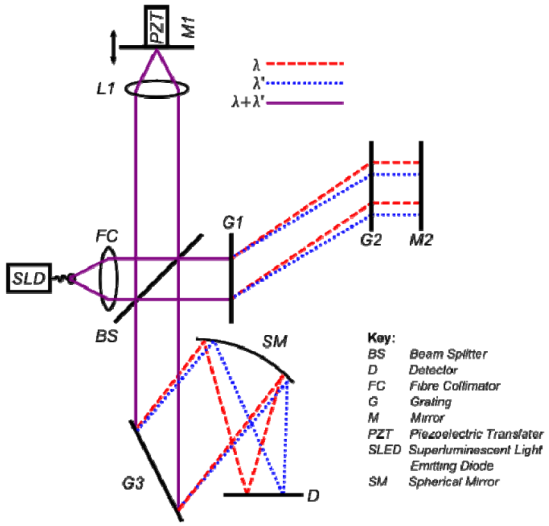

Fig. 1. Schematic diagram of DRI bulk optics interferometer. Upper/lower wavelengths (red/blue) depicted from broader SLED spectrum (purple) where paths are wavelength dependant.

Upon recombination of the measurement and reference beams at the beamsplitter, spectral decomposition is performed by a spectrometer comprising a reflective grating (G3), spherical mirror (SM) and 2048 pixel CMOS line array (D) (ISG Lightwise LW-SLIS-2048A). An example of a typical spectral interferogram obtained from the DRI apparatus is shown in Fig. 2.

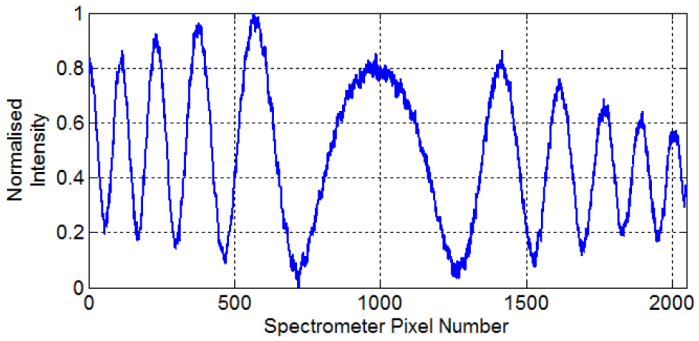

Fig. 2. Spectral interferogram obtained from DRI.

The chromatically dispersed reference light results in a wavelength dependent optical path length in the reference arm. In DRI this results in a spectral interferogram with a stationary phase point which is located at the point of symmetry. The stationary phase point manifests at an equalization wavelength at which the interferometer OPD is zero. The equalization wavelength in turn depends on the measurement arm length, and thus the axial position of the measurand. The absolute position of the measurand may thus be determined by deducing the wavelength of the stationary phase point from the acquired spectral interferogram. The sensitivity of the method is dependent on the amount of chromatic dispersion applied to the reference arm, in addition to the sampling limitations imposed by the fixed pixel number of the line-array spectrometer. However, because DRI is interferometric there is also high resolution phase information present in the interferogram, which if extracted can enhance the axial resolution substantially. The next section describes the use of template matching in order to retrieve this phase information.

#258880 Received 24 Feb 2016; revised 6 Apr 2016; accepted 10 Apr 2016; published 29 Apr 2016

3. Application of template matching

3.1. Overview

Template matching is a well-established technique used in image processing and machine-vision in which the translation of an image subset, known as a template, is carried out across a larger image to find the location of highest correlation between the images and thus a 'match' [11, 12]. For DRI, the template matching strategy is relatively simple because it is essentially a one dimensional problem.

The approach taken was to develop a numerical model of spectral interferogram generation with the DRI apparatus, and then use it to generate a set of simulated template interferograms relating to a range of measurement arm lengths. The advantage of simulated interferograms as templates over real interferograms is due in part to the optimal fringe visibility and lack of noise. In addition, the optical path difference may be altered in much more precise and controlled manner than would be possible in a real apparatus in the presence of environmental noise. With a generated set of template interferograms, each relating to a known OPD and thus axial position, high resolution position information can be extracted from an acquired spectral interferogram using template matching.

Figure 3 summarizes the signal processing operations carried out on the spectral interferograms.

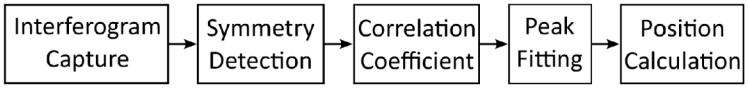

Fig. 3. Flow chart showing template matching signal processing steps.

3.2 Template generation

This section details the creation of a set of n discrete template interferograms, each of length, T. A column vector, k holds a set of discretized wavenumbers representing those sampled by the line-array spectrometer. Here, λ_L is the starting wavelength of the SLD light source, $\Delta\lambda$ is the bandwidth at FWHM, and m is the horizontal pixel count of the CMOS line camera.

$$\mathbf{k} = \left(k_1, \cdots, k_i, \cdots, k_m\right)^T$$
$$\text{where } k_i = 2\pi\left(\frac{1}{\lambda_L} + \frac{i}{\Delta\lambda m}\right) \text{ and } i \in \{1, 2, \cdots, m\} \tag{1}$$

A vector, $\mathbf{r}$ containing the wavenumber dependent optical path is calculated using the grating equation along with the perpendicular grating separation, L and the grating period, D.

$$\mathbf{r} = \left(r_1, \cdots, \mathrm{r}_i, \cdots, \mathrm{r}_m\right)^T \text{ where } \quad r_i = \frac{L}{\sqrt{1 - \left(\frac{2\pi}{k_i D}\right)^2}} \tag{2}$$

It is also necessary to introduce a reference arm offset, d_0 which represents the balancing of the OPD in order to move the stationary phase point of the interferogram to the central wavelength of the spectrometer; in this configuration the gauge can be considered nulled or zeroed. The grating characteristics and the wavelength range used in the DRI apparatus are chosen so that third-order dispersion is negligible and thus a constant rate of change across $\mathbf{r}$ is assumed. In this case, a linear approximation can be made such that,

$$d_0 = r\left(k_c\right) + \alpha k_c - L \tag{3}$$

#258880 Received 24 Feb 2016; revised 6 Apr 2016; accepted 10 Apr 2016; published 29 Apr 2016

$$\alpha = r'(k_c) = \frac{-4\pi^2 L}{D^2 k_c^{\,3}\left[1-\left(\frac{2\pi}{Dk_c}\right)^2\right]^{3/2}} \tag{4}$$

where k_c is the central wavenumber and α is the first differential of the wavenumber dependent optical path length. An m-by-n matrix can then be defined containing the phase function for the DRI at each optical path difference for the set of template interferograms. Each column contains the phase function at a particular OPD. A total of n phase functions are generated spaced at OPD intervals of W .

$$\mathbf{P} = \begin{pmatrix} p_{1,1} & \cdots & p_{1,n} \\ \vdots & \ddots & \vdots \\ p_{m,1} & \cdots & p_{m,n} \end{pmatrix} \text{where } p_{i,j} = 2k_i\left[r_i - L - (W \cdot j) - d_0\right],\ j \in [1,2,\cdots,n] \tag{5}$$

The template interferogram data set is then calculated column-wise. The resulting m-by-n matrix, $\mathbf{H}$, contains n normalised template interferograms each of length m ,

$$\mathbf{H} = \begin{pmatrix} h_{1,1} & \cdots & h_{1,n} \\ \vdots & \ddots & \vdots \\ h_{m,1} & \cdots & h_{m,n} \end{pmatrix} \text{where } h_{i,j} = \frac{1}{2}\left[1+\cos\left(p_{i,j}\right)\right] \tag{6}$$

Each individual template interferogram, $\mathbf{H}_j$ represents an interferogram as captured by the DRI detector across the entire wavenumber range, Δk . The diagram shown in Fig. 4 shows how the interferogram intensity at the point of symmetry evolves as the OPD changes overall several tens of nanometers.

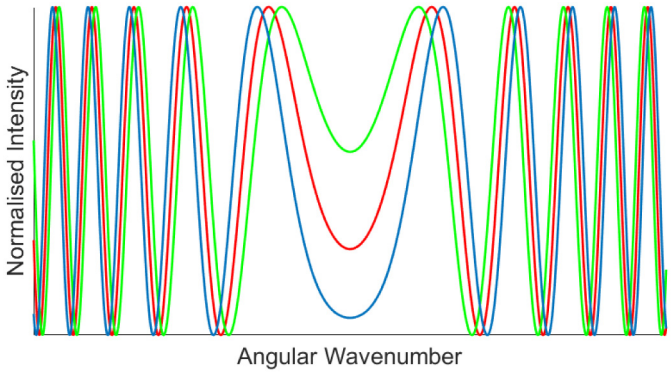

Fig. 4. Three examples of generated template interferograms for consecutive OPD increases of 40 nm.

For the template matching procedure to operate effectively it is not necessary to match the entirety of each template interferogram with the measured interferogram. It is sufficient to compare a subset of the interferograms centered about the point of symmetry. This is beneficial since a reduced number of shorter length template interferograms is required, reducing computational complexity. The template matching procedure continues to operate effectively as the wavenumber at which the point of symmetry, k_v occurs changes throughout the measurement range of DRI. In order to allow this operation across the full range, a rectangular window is applied, effectively cropping the template interferograms. To ensure symmetry of the final templates, the point of symmetry must be calculated and so first,

#258880 Received 24 Feb 2016; revised 6 Apr 2016; accepted 10 Apr 2016; published 29 Apr 2016

autoconvolution is applied to each individual template interferogram, $\mathbf{H}_j$ resulting in a $2m$ by n matrix.

$$\mathbf{C}=\begin{pmatrix} c_{1,1} & \cdots & c_{1,n} \\ \vdots & \ddots & \vdots \\ c_{2m,1} & \cdots & c_{2m,n} \end{pmatrix} \text{where } c_{q,j}=\sum_{i=1}^{m} h_{i,j}\cdot h_{(q-i),j},\ q\in[1,\cdots,2m] \tag{7}$$

Vector $\mathbf{a}$ stores the point of symmetry for each individual template interferogram, $\mathbf{C}_{2i,j}$ which can be determined by storing the index, q denoting the maximally valued element found in the decimated-by-2 column vector.

$$\mathbf{a}=\left(a_1,\cdots,a_j,\cdots,a_n\right) \text{where } a_j=\max\left(\mathbf{C}_{2i,j}\right) \tag{8}$$

To complete the creation of the set of cropped template interferograms, represented as a T by n matrix $\mathbf{H}'$, a rectangular window of even length T, centered on the index value, a_j is applied to each column vector $\mathbf{H}_j$. The operation can be described as follows,

$$\mathbf{H}'=\begin{pmatrix} h'_{1,1} & \cdots & h'_{1,n} \\ \vdots & \ddots & \vdots \\ h'_{T,1} & \cdots & h'_{T,n} \end{pmatrix} \text{where } z\in[1,\cdots,\mathrm{T}]$$
$$h'_{z,j}=h_{\beta,j} \text{where index, } \beta=z+\left(a_j-\frac{T}{2}\right) \tag{9}$$

The red line in Fig. 5 illustrates the calculated center position, a, as well as the portion of the interferogram cropped by the square window resulting in a single column of the matrix $\mathbf{H}'$.

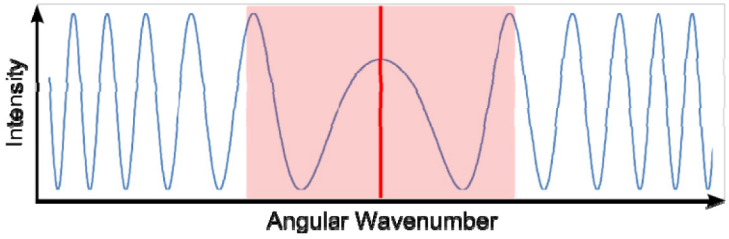

Fig. 5. Template interferograms showing the point of symmetry (red line) as well as the applied rectangular window (red box)

3.3 Template matching

Calculation of the phase of a measured interferogram, $\mathbf{g}$ is achieved by first calculating the interferogram symmetry before application of a rectangular window using the method outlined in Eq. (8) and (9), resulting in a vector, $\mathbf{g'}$, of length T. Figure 6 represents the operation on a acquired interferogram.

#258880 Received 24 Feb 2016; revised 6 Apr 2016; accepted 10 Apr 2016; published 29 Apr 2016

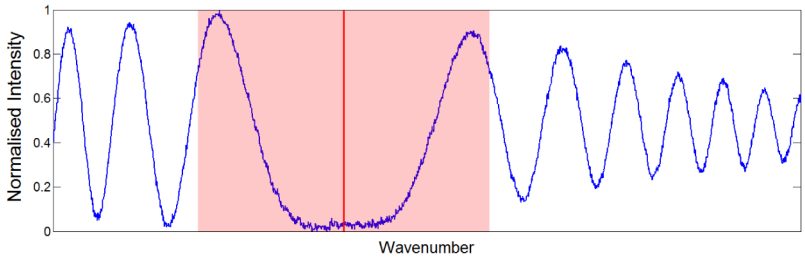

Fig. 6. Interferogram acquired from DRI apparatus with center (red line) and vector $\mathbf{g}'$ (red area) shown.

Next, the correlation coefficient is calculated for $\mathbf{g}'$ and each template interferogram, $\mathbf{H}'_\mathbf{j}$.

$$\mathbf{r} = \left(r_1, \cdots, r_j, \cdots, \mathrm{r}_n\right) \text{ where } r_j = \frac{\mathrm{cov}\left(\mathbf{H}'_j, \mathbf{g}'\right)}{\sigma_{\mathbf{H}'_j}\sigma_{\mathbf{g}'}} \tag{10}$$

The resulting correlation vector, $\mathbf{r}$, contains a peak value with a corresponding index, j_p relating to the location of the the best-matching template in the vector, $\mathbf{H}$. Knowledge of the pre-determined template spacing, W then allows the determination of displacement,

$$z = W \cdot j_p \tag{11}$$

This allows the determination of the displacement with a resolution equal to the template spacing, W. A further enhancement of axial resolution is possible by fitting a polynomial to the correlation vector, $\mathbf{r}$ which enables the deduction of a fractional value of j_p. Empirically, this has the effect of reducing noise in the obtained measurement data and so we employ this method in the presented experimental results.

4. Experimental results

4.1 Overview

The phase calculation method by template matching described in the previous section provides the phase for a single acquired interferogram. In this section an analysis of the DRI apparatus in dynamic terms is presented, in order to ascertain the potential for displacement measurement. The measurement mirror, M1, is mounted on a precision closed-loop piezoelectric translator (Physique Instruments P-721.CLQ) which enables the axial displacement of M1 with a resolution and range of 0.7 nm and 70 µm respectively. The bidirectional repeatability is ± 5 nm.

4.2 Stepwise displacement measurement

Figure 7 shows the calculated displacement from continuously acquired DRI interferograms taken while M1 position was stepped in 10 nm increments through a range of 1 µm. The 10 nm steps are clearly resolved confirming the potential for the template matching method for resolving high resolution position information. It is apparent that unlike our previously reported absolute displacement method [10], the high resolution phase information is a relative measurement with the phase wrapping around every $\lambda/2$ nm, this in order to make measurements of larger displacements the phase must be tracked and unwrapped.

#258880 Received 24 Feb 2016; revised 6 Apr 2016; accepted 10 Apr 2016; published 29 Apr 2016

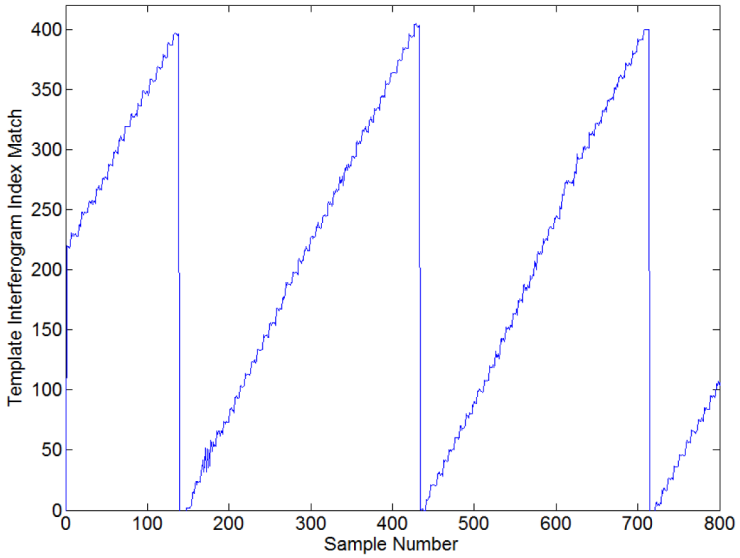

Fig. 7. Phase calculated for real interferograms as the measurement mirror M1 is advanced by 10 nm steps at 2 Hz.

The full axial measurement range over which phase can be tracked is limited by three factors. First, it is necessary that the rectangular window applied to the acquired interferogram using Eq. (9) is not truncated at the edge of the data set as the stationary phase point moves toward the detector edges. Second, the ability of the autoconvolution algorithm to detect interferogram center deteriorates as the center approaches the detector edges. Finally, the physical attributes of the bulk optics interferometer (dispersion, source bandwidth) influence the interferogram shape and the rate of change of interferogram center position with OPD change. These three factors enable a range of 350 μm for an experimental setup using gratings having a period, D of $D = 3\times10^{-5}$ m and a separation, $L = 330$ mm and a source having a linewidth of 25 nm.

4.3 Noise floor estimation

In order to assess the noise floor of the DRI apparatus to enable an estimation of axial resolution, 1401 interferograms were acquired over a period of 60 seconds, with the mirror in a fixed position. The apparatus was situated in an enclosure on a vibration isolating optical table to minimize environmental effects. Figure 8 shows calculated position data acquired from the DRI and a fitted polynomial used to remove the low frequency drift due to temperature that is readily apparent. Figure 9 shows the calculated residuals from the fitting and represents the actual noise floor. Figure 10 shows that the noise distribution is Gaussian and has a standard deviation of 0.63 nm. No averaging was applied to the data in order to obtain these results.

#258880 Received 24 Feb 2016; revised 6 Apr 2016; accepted 10 Apr 2016; published 29 Apr 2016

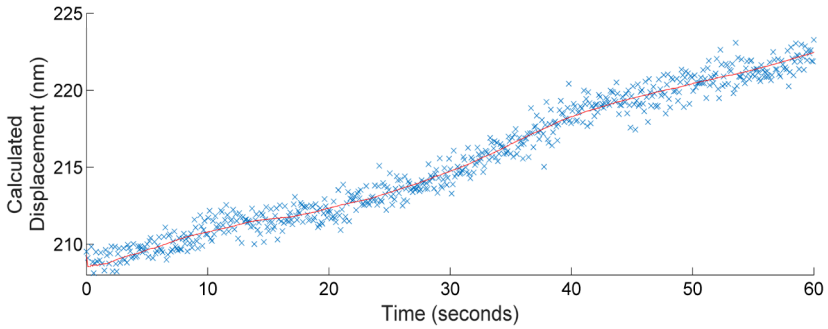

Fig. 8. Data taken over 60 seconds in a free-running steady-state showing temperature drift. Polynomial fit (red line) taken to allow drift removal.

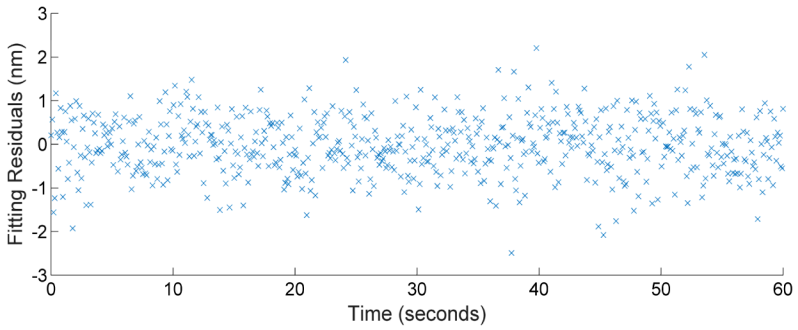

Fig. 9. Residuals from polynomial fit on data shown in Fig. 8.

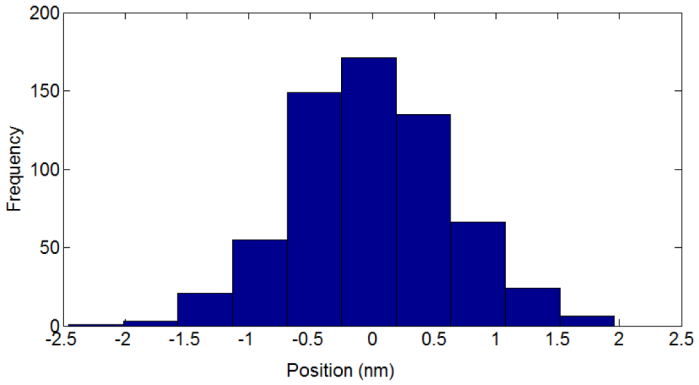

Fig. 10. Histogram of data presented in Fig. 9 demonstrating a Gaussian noise distribution.

4.4 Linearity

A study of the linearity of the axial position measurement from the DRI apparatus was performed by translating M1 axially through a 60 μm range in 20 nm steps at a rate of 2 Hz. The calculated phase was unwrapped before the displacement was calculated in order to continuously track the mirror translation. Figure 11 shows the residuals resulting from a linear fit taken through the calculated position data. A resulting integral nonlinearity of approximately 40 nm is discernable looking at the general trend. The source of the non-linearity can be attributed primarily to two factors which at present are inseparable. First, drift in the interferometer caused by environmental disturbances, the whole measurement cycle took approximately 2000 seconds. Second, there is a quoted integral non-linearity of 20 nm in

#258880 Received 24 Feb 2016; revised 6 Apr 2016; accepted 10 Apr 2016; published 29 Apr 2016

the manufacturers specification for the PZT which represent over half of the quantity measured.

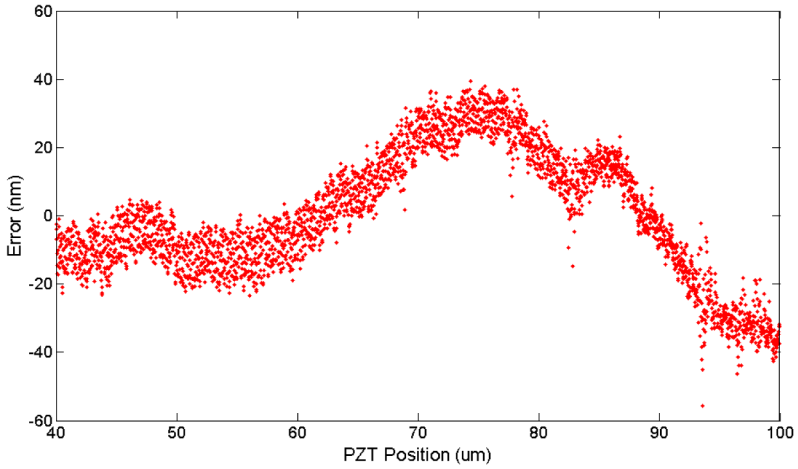

Fig. 11. Residuals from a linear fit taken through calculated displacement data across a 60 µm axial mirror translation in 20 nm steps.

4.5 Measurement repeatability

The measurement repeatability was ascertained by toggling the axial position of the measurement mirror between two positions, 100 nm apart. The difference between the two calculated axial positions was taken for each run, which enables the effect of temperature drift to be negated. A total of 100 runs were recorded over the course of were made over ~110 seconds which corresponds to the shortest time that still ensured the sufficient mechanical settling of the PZT after each translation. Figure 12 shows a histogram plot of this data, which shows a Gaussian distribution, with a standard deviation of 1.25 nm.

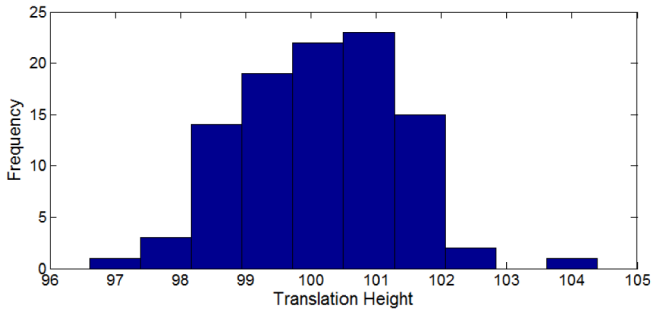

Fig. 12. Histogram showing measured step height position for 100 nm rising steps repeated 100 times.

4.6 Phase-order determination for high-resolution absolute displacement measurement

In this section we demonstrate the potential for high dynamic range displacement measurement in DRI by using previously reported absolute (wavelength encoded) displacement data [10] to determine the phase-order of the high resolution (phase encoded) data extracted using template matching. This requires a calibration process in which the measurement mirror (M1) is translated continuously while recording spectral interferograms. Figure 13 shows a resulting data set over ~10 phase wraparounds. The relative displacement calculated by template matching is shown in blue. The absolute displacement, encoded by wavelength as the spectrometer pixel position at which the point of symmetry occurs, is

#258880 Received 24 Feb 2016; revised 6 Apr 2016; accepted 10 Apr 2016; published 29 Apr 2016

shown in green. The positions of the phase wraparounds in the high resolution relative data are determined by taking the first derivative and then locating the minima. A map of the absolute pixel positions at which the phase wraparound occurs are then stored in a look-up table which may be recalled later to enable phase-order determination.

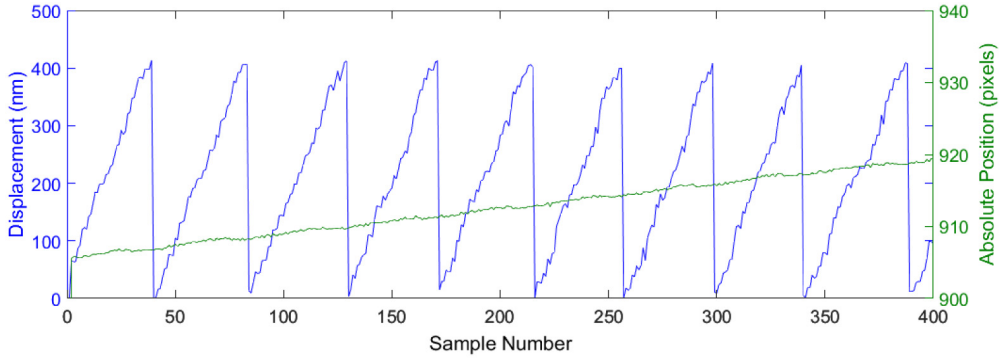

Fig. 13. High-resolution displacement data obtained by template matching (blue), combined with absolute displacement data determined by the spectrometer pixel position of the interferogram point of symmetry (green) during an axial scan of mirror M1.

Figure 14 shows the phase order determination in operation across an axial mirror translation over an ~8 μm range. The blue trace shows the raw wrapped phase data optained using template matching. The red trace shows the phase-order multipler value as determined by the mapping process, each stepwise increment represents a change in phase-order. The black trace is the final displacement measurement using the high resolution phase-encoded data in which the phase-order has been successfully determined, yielding an absolute measurement result.

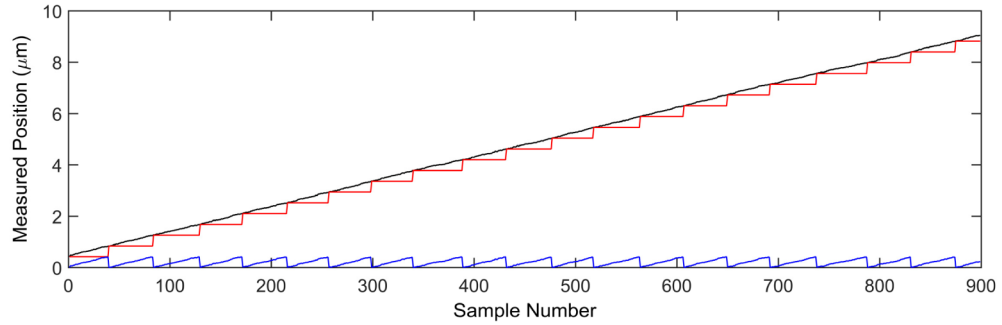

Fig. 14. Absolute position determination (black) from the original ambiguous high-resolution template matching data (blue) using the phase-order multipler map (red) determined by the calibration process.

This method of determining the phase order requires a lengthy calibration procedure involving the scanning of the mirror through the full axial measurement range. Further work will investigate numerical approaches based upon further optimization of the simulation model to more accurately represent the DRI as well as more analytical approaches.

5. Conclusion

This paper describes the use of template matching as a signal processing technique to calculate optical path difference, and thus displacement, from a dispersed reference interferometer (DRI). The experimental results presented show that this method is able to achieve nanometer resolutions with the current noise floor. Evaluations of the measurement repeatability further strengthen the case for high resolution displacement measurement.

#258880 Received 24 Feb 2016; revised 6 Apr 2016; accepted 10 Apr 2016; published 29 Apr 2016

Finally, a method for deriving the phase-order of the the high-resolution measurement using absolute (wavelength encoded) position information from the spectral interferogram was described. It is worth reiterating that the data presented in this paper is presented as acquired, with no oversampling or averaging as commonly performed with high resolution measurements. It is envisaged that further performance improvements will be achieved through the application of fringe regularization techniques to correct the systematic distortions in the acquired spectral interferograms which result primarily from the spectral responses of the SLD and spectrometer.

Template matching, when coupled with previously reported absolute positioning methods [10] has the potential to yield very high dynamic range measurement though the ability to resolve nanometre scale displacements. In contrast to comparable point-sensing techniques such as chromatic confocal sensing, DRI is an interferometric technique with inherently high sensitivity and as such does not rely on oversampling to reach nanometre measurement precisions. This leads to the possibility of higher measurement rates for a given measurement precision. Furthermore, the DRI apparatus is of comparable complexity and cost as that used for chromatic confocal sensing. Further work to optimize the optics in the measurement arm to form a probe will allow the potential of DRI for high dynamic range surface profilometry to be fully evaluated.

Acknowledgments

The authors gratefully acknowledge the UK's Engineering and Physical Sciences Research Council funding of the Center for Innovative Manufacturing in Advanced Metrology (EP/I033424/1) and the European Research Council Surfund Project (ERC-228117).

#258880 Received 24 Feb 2016; revised 6 Apr 2016; accepted 10 Apr 2016; published 29 Apr 2016